Complex evolutionary dynamics govern the diversity and distribution of biosynthetic gene clusters and their encoded specialized metabolites

Alexander B. Chase[1], Douglas Sweeney[1,2], Mitchell N. Muskat[1], Dulce Guillén-Matus[1,2], and Paul R. Jensen[1,2]

[1]Center for Marine Biotechnology and Biomedicine, Scripps Institution of Oceanography, University of California, San Diego, California
[2]Marine Biology Research Division, Scripps Institution of Oceanography, University of California, San Diego, California

ABSTRACT While specialized metabolites are thought to mediate ecological interactions, the evolutionary processes driving their distributions, particularly among closely related lineages, remain poorly understood. Here, we examine the evolutionary dynamics governing the diversity and distribution of biosynthetic gene clusters (BGCs) in 118 strains across nine described species within the marine actinomycete genus *Salinispora*. While previous evidence indicated that horizontal gene transfer largely contributed to BGC diversity, we find that a majority of BGCs in *Salinispora* genomes are maintained by processes of vertical descent. In particular, we identified species-specific signatures that were associated with both BGC distributions and the production of their encoded specialized metabolites. By analyzing nine experimentally characterized BGCs that range in conservation from species to genus specific, we find that the distribution of BGCs among *Salinispora* species is maintained by selection, while BGC diversification is constrained by recombination among closely related strains and strengthened by gain/loss events between species. Notably, the evolutionary processes driving BGC diversification had direct consequences for compound production, elucidating the mechanisms that lead to chemical diversification. These results support the concept that specialized metabolites, and their cognate BGCs, represent functional traits associated with ecological differentiation among *Salinispora* species.

GRAPHICAL ABSTRACT

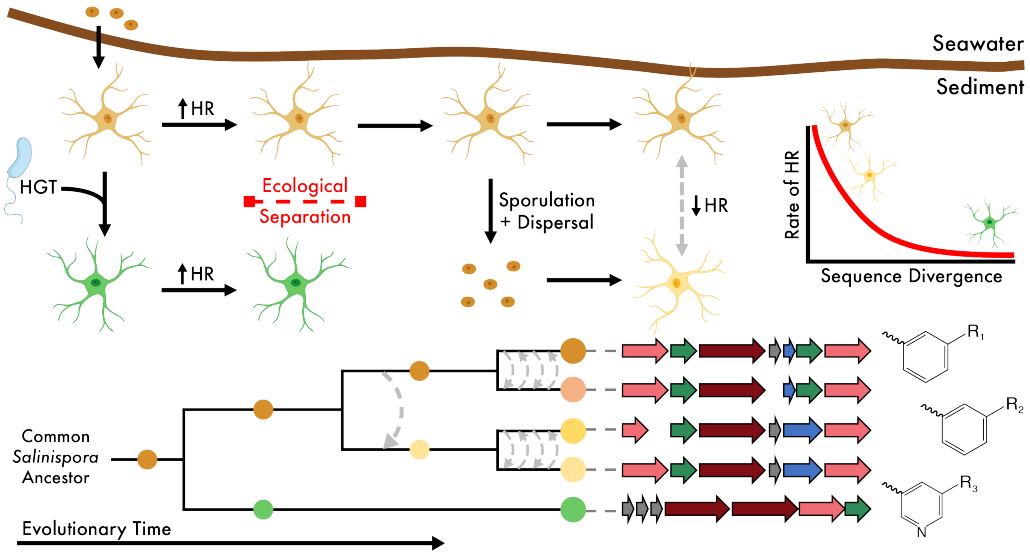

KEYWORDS *Salinispora*, vertical inheritance, homologous recombination, microbial ecology, speciation

Complex evolutionary dynamics govern the diversity and distribution of biosynthetic gene clusters and their encoded specialized metabolites

Alexander B. Chase[1], Douglas Sweeney[1,2], Mitchell N. Muskat[1], Dulce Guillén-Matus[1,2], and Paul R. Jensen[1,2]

[1]Center for Marine Biotechnology and Biomedicine, Scripps Institution of Oceanography, University of California, San Diego, California
[2]Marine Biology Research Division, Scripps Institution of Oceanography, University of California, San Diego, California

Salinispora | vertical inheritance | homologous recombination | microbial ecology | speciation

INTRODUCTION

Despite linkages between abiotic factors and bacterial diversity (1–3), the key functional traits driving biotic interactions in microbial communities remain poorly understood. These functional traits likely include specialized metabolites, or small molecule natural products, that are known to modulate ecological interactions between organisms (4). Specialized metabolites, which include antibiotics and siderophores, can drive biotic interactions via mechanisms such as competition, nutrient uptake, and defense, and thus likely represent a major driver of microbial community composition (4). Given that microbes produce a wide variety of biologically active natural products, these compounds may contribute to the diversification and environmental distribution of microbes, as has been observed in eukaryotes (5). To date, however, studies of bacterial specialized metabolite production have largely focused on the discovery of compounds with pharmaceutical potential as opposed to understanding their ecological and evolutionary significance.

Marine sediments represent a unique environment to assess the relationships between microbial diversity and specialized metabolite production. Sediments are associated with diverse microbial communities (6) where competition for limited resources is facilitated via the secretion of small molecules (7, 8). Among bacteria inhabiting marine sediments, actinomycetes such as the genus *Salinispora* are well-known for the production of specialized metabolites (9–11). *Salinispora* (family: Micromonosporaceae) is a member of the rare biosphere in surface sediments (12) and can readily be cultured from tropical and sub-tropical locations (13). This relatively recently diverged lineage includes nine closely related species that share >99% 16S rRNA sequence similarity (14). The presence of this "microdiversity" suggests that fine-scale trait differences contribute to differential resource utilization and niche partitioning (15, 16). Indeed, two *Salinispora* species were recently shown to employ differential ecological strategies for resource acquisition (17), providing insights into the ecological and evolutionary mechanisms contributing to *Salinispora* diversification.

While *Salinispora* has proven a robust model for natural product discovery (18), much remains to be resolved concerning the evolutionary dynamics of the biosynthetic gene clusters (BGCs) encoding these compounds. Prior analyses of *Salinispora* BGCs revealed extensive horizontal gene transfer (HGT) and exchange both within and between species (19), suggesting a "plug and play" model of BGC evolution (20). The exchange of BGCs among *Salinispora* species is likely mediated by conjugative elements, as in *Streptomyces* (21), and further facilitated by the absence of geographic barriers in their distribution (22). At the same time, profiles for the production of specialized metabolites encoded by *Salinispora* BGCs revealed species-specific patterns (23), providing competing models for BGC evolution.

Resolving the evolutionary dynamics driving BGC distributions in *Salinispora* can help inform future natural product discovery efforts. By one account, the horizontal exchange of *Salinispora* BGCs may be frequent and highly dependent on the local community (19, 20), resulting in similar strains from different locations yielding different metabolites. Alternatively, the small molecules encoded by some BGCs may represent traits driving ecological differentiation (23, 24), in which case these BGCs should remain phylogenetically conserved. To reconcile these seemingly contrasting scenarios, we sought to identify the evolutionary processes contributing to the distribution of BGCs. We hypothesized that specialized metabolite production is subject to strong selective pressures, with compounds and their associated gene clusters representing functional traits contributing to ecological differentiation. If correct, we expected the distribution of BGCs, regardless if they were horizontally acquired at some point in time (19), to be subsequently maintained within *Salinispora* through processes of vertical descent. To better understand the role of vertical inheritance in driving BGC evolution, we revisited the distribution of BGCs in 118 genomes across the nine described *Salinispora* species (14). Finally, to assess the functional consequences of BGC diversification on compound production, we focused on nine experimentally characterized BGCs and applied targeted tandem mass spectrometry to detect their associated molecules. Our results support the hypothesis that specialized metabolites represent functional traits contributing to ecological differentiation among closely related *Salinispora* species.

RESULTS

Salinispora species delineated by biosynthetic potential

To gain insight into the functional traits that differentiate the nine *Salinispora* species (14), we first assessed the composition of the core and flexible genomes. Based on species designations and our core genome phylogeny (Figure 1A), we expected strains within the same species to share more flexible genes than strains between species. Indeed, flexible gene similarity was highly congruent with species designations (Figure 1B), with strains within the same species sharing more flexible genes than expected by chance (Mantel R=0.91; p<0.001). Geographic location, to a lesser degree, also contributed to flexible gene

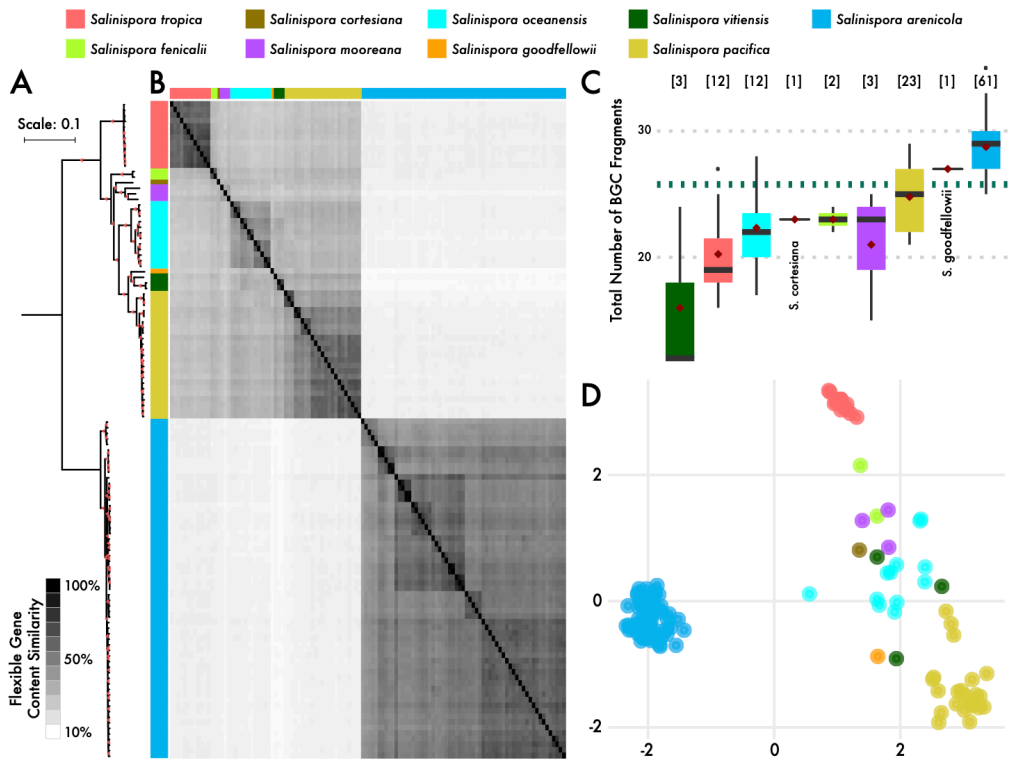

Figure 1. Genetic relatedness of globally-distributed *Salinispora* strains (N=118).
A) Core genome phylogeny based on a concatenated alignment of core genes. Colors denote species. Bar, 0.1 nucleotide substitutions per position. Bootstrap values indicate >90% support.
B) Flexible gene content similarity between strains. Heatmap was generated from a Jaccard distance matrix.
C) Total number of biosynthetic gene cluster (BGCs) fragments identified across *Salinispora* species. Black bar represents median distribution, red diamond represents mean distribution. Dashed line denotes genus average. N represents number of genomes per species.
D) Non-metric multidimensional scaling (NMDS) plot depicting gene cluster family (GCF) composition for each *Salinispora* strain. Circles represent strains colored by species.

composition (Mantel R=0.06; $p<0.05$). Within the flexible genome, we also identified species-specific orthologs (defined as genes shared by all strains within a species but not observed in any other *Salinispora* species). These genes, which should provide insights into the functional traits that distinguish *Salinispora* species, were largely annotated as hypothetical proteins (Figure S1A). Of the available annotations, 18.1±15.3% of the species-specific orthologs were associated with specialized metabolism (Figure S1B). In addition, when we searched the genomic regions flanking all species-specific orthologs, regardless of annotation, we found that 28.9±26.2% were located within the boundaries of predicted biosynthetic gene clusters (BGCs; Figure S1C).

Given the large percentage of species-specific flexible genes associated with specialized metabolism, we expected that BGC diversity and distribution would similarly correlate with *Salinispora* species diversity. To address this, we first identified a total of 3041 complete or fragmented (on contig edges) BGCs across all 118 *Salinispora* genomes (mean = 25.8 per genome) accounting for 18±2.3% of an average 5.6 Mbp *Salinispora* genome. When compared to other bacterial genera, including taxa well-known for specialized metabolite production (e.g., *Moorea* and *Streptomyces*), *Salinispora* dedicated the highest genomic percentage to this form of metabolism (Figure S2), further highlighting its importance in this genus. When we compared BGCs between *Salinispora* species, we observed significant variation in the total number of BGCs (Figure 1C; analysis of variance [ANOVA]; $p<0.001$) and the genomic percentage dedicated to specialized metabolite production (Figure S2; ANOVA; $p<0.001$). In cases where the number of genome sequences are low (e.g., *S. vitiensis*), BGC abundances may not be representative of the species.

To compare BGC composition across species, we grouped the 3041 predicted BGCs into 305 gene cluster families (GCFs; Figure S3A). Similar to prior reports (20), 35% of the GCFs were populated by a single BGC (Figure S3B). It can be inferred that these BGCs represent relatively recent acquisition events including local adaptations that are not well represented in our genomic dataset. Despite representing a large percentage of the total GCF diversity, the singleton BGCs comprised only 3.6% of the BGCs detected among all strains (108 out of 3041) and equate, on average, to only 0.9 BGCs per *Salinispora* genome (inset Figure S3B). In contrast, the vast majority of BGCs were shared among strains (Figure S3C). As in flexible gene content, we found that 77% of the variation in GCF composition was explained by species designation (Figure 1D; reporting Mantel R; $p<0.001$), with geography explaining an additional 5% (reporting Mantel R; $p<0.05$). Correlations between BGC distributions and species delineations are further supported by BGC average nucleotide identity (ANI) values, which were highly similar to the whole-genome ANI values used to delineate species boundaries (Figure S4). Nonetheless, a small percentage of shared BGCs (1.4%) showed evidence of interspecific transfer (Figure S4B). Collectively, these results indicate that HGT events provide a mechanism to expand BGC diversity, while at the same time, BGC composition is largely driven by processes of vertical descent.

Table 1. Recombination, duplication, transfer, and loss events of nine BGCs relative to the core genome.

				Recombination Metrics				DTL Model Predicted Events			
BGC	Num. of Species	Num. of strains	Alignment Length (bp)	R/θ	δ	v	r/m	Interspecific Transfer	Intraspecific Transfer	Duplication	Loss
lom	6	42	84964	0.016	6696.0	0.026	2.77	0	10	0	14
lym	9	109	32597	0.019	4101.2	0.021	1.63	0	33	1	33
rif	1	59	91550	0.655	6368.3	0.003	13.90	0	23	0	15
sal	6	30	15911	0.024	3453.9	0.032	2.70	2	5	0	16
slc	2	25	31937	0.020	1316.7	0.058	1.57	1	11	1	5
slm	3	25	28111	0.189	428.0	0.041	3.28	1	10	0	14
spo	2	13	167237	0.018	1032.6	0.093	1.71	1	5	0	3
spt	7	112	13368	0.904	1115.5	0.010	10.16	3	49	0	22
sta	4	77	19319	0.069	1352.4	0.032	2.96	0	22	1	23
Core Genome	9	28	4668606	0.061	1111.6	0.026	1.75				

R/θ = relative rate of recombination to mutation
δ = mean import length of recombining DNA
v = mean divergence of imported recombining DNA
r/m = relative impact of recombination to mutation accumulation on per-site substation rate (equal to R/θ * δ * v)

Drivers of BGC distribution and diversity

Given that BGC distributions are largely explained by shared phylogenetic history, we sought to identify the specific evolutionary processes acting on BGCs that have been maintained through vertical inheritance. To do so, we selected nine GCFs that range in conservation from species-specific to nearly ubiquitous in the genus (Table S2). Representative BGCs within all nine GCFs have been experimentally characterized (Figure S5) (25–33) allowing for direct associations between BGC evolution and its consequences for metabolite production.

Phylogenies of the nine BGCs (Figure S6) indicated that their genetic distances were a function of divergence time (Figure 2; multiple R^2 = 0.89, p<0.001). While BGC diversification largely coincided with core genome divergence, an event-inference parsimony model indicated that a variety of evolutionary processes, including BGC duplication, transfer, and loss events, contributed to the observed BGC distributions (Table 1). In particular, there were frequent intraspecific transfers, averaging 18.7±14.7 across the nine BGCs, relative to interspecific transfers (0.9±1.1), supporting the ANI result that BGCs are rarely transferred between species (Figure S4). In the few cases where interspecies transfers occurred (e.g., *spo* and *slc* BGCs), the BGCs remained monophyletic post-transfer (Figure S6) and their genetic divergence remained a function of the core genome (Figure 2), supporting a single transfer event followed by vertical inheritance. The model further revealed that BGC loss events (Table 1) explained the patchy distributions of some BGCs. For instance, the *lom* BGC followed a strict model of vertical inheritance with predicted loss events in *S. mooreana* and *S. oceanensis* (Figure S6). Together, these results indicate that diversification in the nine BGCs is highly correlated to divergence time with frequent intraspecies recombination and loss events.

To better understand the impact of recombination in structuring the genetic diversity within the nine BGCs, we calculated the ratio at which nucleotides are replaced by either recombination or point mutations (*r/m*). At the genome level, high levels of recombination (Table 1; *r/m*=1.8) among closely related strains (v=0.03 or 3% genetic divergence among strains) maintains genetic cohesion within species. In fact, a recombination network revealed no recent gene flow between recombining populations within Salinispora species (Figure S7) suggesting this genetic isolation may be evidence of nascent speciation events. Similarly, at the BGC level, high levels of recombination (all *r/m*>1.5) were restricted to events between closely related strains (v_{MEAN} = 3.5%; Table 1). For example, recombination in the *rif* BGC (*r/m*=13.9) was restricted to strains that have diverged by <0.3%. Recombination events were also restricted in the size of their recombining segments, as the average length of a recombining segment (δ) was a fraction of the total BGC length (Table 1). Finally, these events had varying effects on the genetic diversity of the nine BGCs. For instance, the two most widely distributed BGCs, *lym* and *spt*, exhibited drastically different *r/m* values (1.6 and 10.2, respectively). As a result, reduced recombination allowed the *lym* BGC to evolve in accordance with the core genome, while frequent recombination of the *spt* BGC limited its divergence (Figure 2). While recombination can homogenize genetic diversity, these events were limited to small sections of the BGCs.

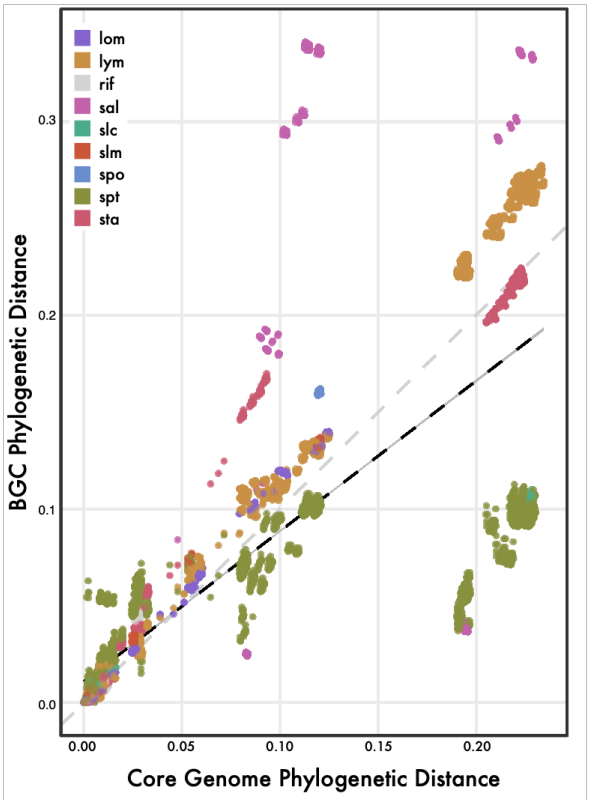

Figure 2. Phylogenetic distances of biosynthetic gene cluster (BGC) and the core genome.
Each point represents a pairwise comparison between a BGC and its core genome, colored by the BGC. Null expectation of neutral divergence in gray (ratio of 1:1 divergence), with total regression line in black.

Homologous recombination can also facilitate gene-specific sweeps (34), which can be evident by reduced nucleotide diversity. A comparison of the conserved biosynthetic genes found in the nine BGCs with those found in the core genome revealed reduced nucleotide diversity in the *sal* and *spo* BGCs in *S. pacifica* and the *slc* BGC in *S. arenicola* (Figure S8A). However, the BGCs in these three instances were only observed in a small number of closely related strains (i.e., three *S. pacifica* and five *S. arenicola* strains sharing >99.6% and >99.4% genome-wide ANI, respectively), which likely accounts for the reduced diversity. In contrast, most conserved biosynthetic genes showed no evidence of recent selective sweeps, with the relatively high nucleotide diversity indicating that recombination was insufficient to prevent BGC diversification. Depressed gene flow observed in the recombination network (Figure S7) provides further support that recombination is unlikely to constrain species-level BGC diversification. Notably, this diversification was neutral based on analyses of selection coefficients (dN/dS). Among the 134 conserved biosynthetic genes analyzed, 97.8% had dN/dS<1, indicating neutral, nondirectional selection (Figure S8B). Thus, it appears that the high nucleotide diversity in *Salinispora* BGCs, such as *rif* (Figure S8A), is due to ancestral sweep events followed by neutral divergence and constrained recombination.

Specialized metabolites as functional traits

We next sought to determine how the evolutionary dynamics driving BGC diversification translated to compound production. Using untargeted liquid chromatography, high-resolution tandem mass spectrometry (LC-MS/MS), we detected 3575 unique molecular features from 30 representative strains across the nine *Salinispora* species. After dereplication, strains within the same species produced more similar molecular features than strains between species (Figure 3A; PERMANOVA; $p<0.01$), with 44.9% of the variation explained by species designation. These results, in combination with GCF composition (Figure 1D), provide clear evidence that vertical descent plays a major role in structuring *Salinispora* specialized metabolism.

At some level, the genetic diversity observed within GCFs should translate into structural differences in the compounds produced. Considering the nine BGCs analyzed above, we noted genetic differences ranging from single nucleotide polymorphisms (SNPs) to variations in gene content. To address how these changes may affect compound production, we used targeted metabolomics to detect compounds previously reported from the nine BGCs. In total, we detected 25 known compounds and many putative analogs in the culture extracts (Table S3). The presence of a BGC did not always equate to product detection (i.e., salinichelins and salinipostins were not detected), suggesting the culture or extraction methods may not have been appropriate. However, the products of seven BGCs were detected, with strains from the same species preferentially producing similar compounds and analogs (Figure 3B; PERMANOVA, $p<0.01$). These results indicate that BGC diversification largely affects compound production at the species level and highlight the importance of accurate species designations when considering BGC evolution.

Importantly, the genetic differences associated with BGC diversification varied in their impact on metabolite production. At the genetic level, the relatively high intraspecies nucleotide diversity observed within the *rif* BGC in *S. arenicola* (Figure S8A) did not reflect differences in rifamycin production (Figure 3B). This diversity, which was considered neutral in terms of dN/dS values, does not affect compound production, and thus indicates that strong selective pressures operate to maintain production of the potent antibiotic rifamycin S in *S. arenicola*. Conversely, subtle differences in auxiliary gene content in the *sta* BGC affected compound production. While three of the four species that encode this BGC produced staurosporine, *S. mooreana* preferentially produced 7-hydroxystaurosporine (Figure 3B). Comparative genomics revealed that the NAD-dependent dehydratase enzyme is missing in the *S. mooreana sta* BGC (Figure S9A), which could account for the presence of the hydroxy group in the molecule produced by this species (Figure S5). More pronounced interspecies polymorphisms were

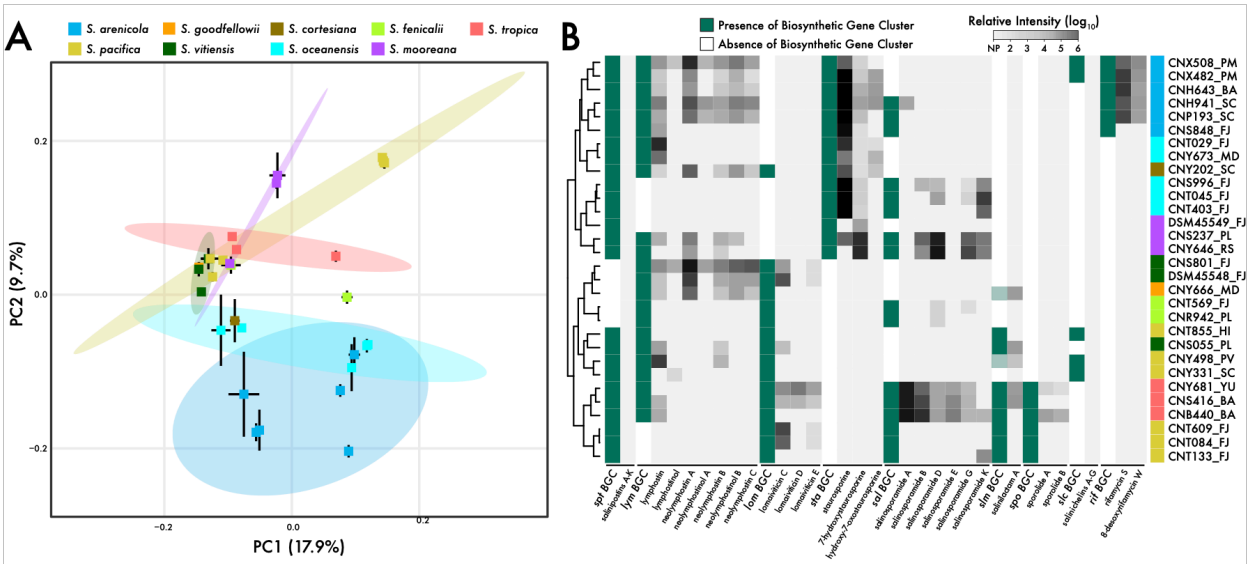

Figure 3. *Salinispora* metabolomics and BGCs distributions across nine species (N=30 strains).
A) Principal Components Analysis (PCA) showing relationship among strain metabolomes. Each point represents a strain colored by species. Standard deviations shown as black lines for each strain and ellipses as 95% confidence intervals for each species.
B) Targeted analysis for the products of nine BGCs. Hierarchical clustering of the relative production of analogs generated from a Euclidean distance matrix. Green/white bars show the BGC presence/absence. Light green bars indicate the detection of a BGC fragment. Gray/black bars show the relative production of each identified analog, NP=no production. x-axis lists BGC name followed by product names. y-axis lists strains colored by species with abbreviations for geographic origin (BA=Bahamas, FJ=Fiji, HI=Hawaii, MD=Madeira Islands, PL=Palau, PM=Palmyra, PV=Puerto Vallarta, RS=Red Sea, SC=Sea of Cortez, YU=Yucatan).

observed in the *spo* BGC between *S. tropica* and the subset of *S. pacifica* strains (3 of 23) that possess the BGC. While all strains maintain the type I polyketide synthase (PKS) responsible for the polyketide core (33), the three *S. pacifica* strains lack the 45 kbp nonribosomal peptide synthetase (NRPS) region responsible for attachment of the cyclohexenone epoxide unit (Figure S9B). Correspondingly, the *S. pacifica* strains did not produce sporolides (Figure 3B) or any other derivatives that could be identified. Interestingly, the 20 *S. pacifica* strains that lack the *spo* BGC encode a similar enediyne BGC linked to cyanosporaside production (19), suggesting the products may perform similar ecological functions. Together, these results directly link BGC diversification to structural changes in the encoded metabolites.

Salinosporamide: a case study for BGC evolution

To further illustrate the evolutionary processes driving chemical diversification, we examined the *sal* BGC, which encodes the biosynthesis of the anti-cancer agent salinosporamide A and analogs (25, 35). While salinosporamides A and K were originally reported from *S. tropica* (36) and *S. pacifica* (35, 37), respectively, we now show that the *sal* BGC is observed in six of the nine *Salinispora* species (Figure 4A). Phylogenetic analysis provides evidence that the *sal* BGC was transferred relatively recently between *S. arenicola* and *S. tropica* (Figure 4A) but has otherwise descended vertically within the genus (Figure S6). Notably, the *sal* BGC is rapidly diverging with respect to the core genome (Figure 2), while at the same time being highly conserved at the species level (Figure S10). Thus, the *sal* BGC provides a useful model to address the relationships between species diversification, BGC composition, and compound production.

We performed targeted metabolomics on 16 strains encoding the *sal* BGC across the six *Salinispora* species (Table S3). All strains maintain the biosynthetic genes responsible for the core γ-lactam-β-lactone ring (*salABCDEF*) and the cyclohexenylalanine amino acid residue, although the position of the latter varied (Figure 4B). While 15/16 strains produced detectable amounts of salinosporamides, the analogs and their yields varied across species (Figure 4C; ANOVA, $p<0.01$). *S. tropica* and *S. arenicola* were the only species in which salinosporamide A was detected and they are the only species to possess the 15kbp region of the BGC responsible for assembly of the chloroethyl-malonyl-CoA extender unit (Figure 4B) (25). This is the first report of salinosporamide A production in *S. arenicola*, although the presence of the BGC in this species was previously documented (20, 38). While the *sal* BGCs in *S. tropica* and *S. arenicola* are nearly identical (e.g., *salA* and *salB* genes share 95.1% and 97.5% amino acid sequence identity between species, respectively), the production of salinosporamides in *S. arenicola* was reduced relative to *S. tropica* (Figure 4C; note log scale). This could be due to a splicing event in the overlapping coding regions in *salDE* (Figure 4B), which may render *salE*, a chaperone MbtH-like protein in NRPS biosynthesis (39), inactive.

Molecular networking provided additional insights into species-specific patterns of salinosporamide production (Figure S11). Here, we detected potentially new salinosporamide derivatives, including one (*m/z* 307.154) produced exclusively by *S. mooreana*. Inversions of the cyclohexenylalanine amino acid encoding region of the *sal* BGC in *S. mooreana* and *S. fenicalli* (Figure 4B) could facilitate novel structural modifications by down-stream auxiliary genes (Figure S10). The network also revealed evidence that salinosporamide analog production varied by species. We investigated this by analyzing the C-2 γ-lactam side chain and found that *S. tropica* and *S. arenicola* produced compounds with the largest R-groups (Figure 4C). This results from the incorporation of chloroethyl-CoA or propyl-malonyl-CoA extender units yielding salinosporamides A and E, respectively (25). Similarly, *S. fenicalii* and *S. mooreana* preferentially produce salinosporamides B and D with medium sized R-groups, while *S. oceanensis* and *S. pacifica*

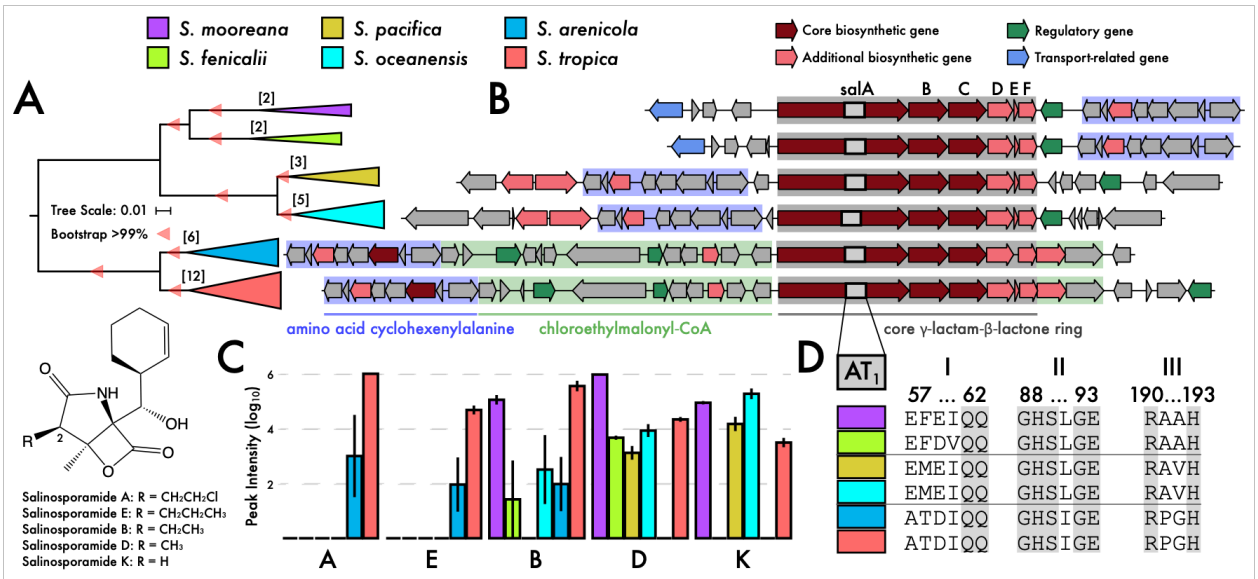

Figure 4. Variations in the salinosporamide BGC (*sal*) and its products.
A) Phylogeny of the *sal* BGC. Colors denote species. Bar, 0.01 nucleotide substitutions per position. Bootstrap values indicate >99% support. Brackets indicate number of genomes in each species encoding the BGC.
B) Representative BGC for each species. Genes are colored by predicted biosynthetic function with gene blocks colored by their role in compound production.
C) Salinosporamides production across species. Analogs are listed in descending order based on R-group side chain size.
D) Sequence alignments of the *salA* AT_1 domain showing three signature motifs associated with substrate specificity. Conserved amino acid regions in grey.

preferentially produce salinosporamide K, which has the smallest R-group. Based on these observations, we suspected substrate discrimination by the *salA* PKS acyltransferase domain (AT_1). Indeed, the three signature motifs related to extended unit specificity (35) were highly conserved at the species level and strongly associated with the length of the C-2 R-group in the salinosporamide product (Figure 4D, Figure S12). Structural protein modelling of the AT_1 domain identified motif I (amino acid residues 57-59) as a novel extension of the active site that possibly allows for extender unit discrimination (Figure S13A). In this case, the smaller, polar residues (Ala57 and Thr58) in *S. tropica* and *S. arenicola* (Figure S13B) could accommodate larger substrates yielding salinosporamides A and E, while the larger residues observed at these positions in other species may not. Thus, salinosporamide production is likely affected not only by the ability to synthesize the various extender units but also recognition and selection of the appropriate substrate by the AT_1 domain.

DISCUSSION

It has become increasingly clear that the fine-scale genomic diversity observed in microbial communities reflects the large number of ecologically distinct lineages that co-occur within microbiomes (40–42). At the same time, the phenotypic traits that allow for the coexistence of closely-related lineages remain less clear (15). By analyzing strains from the recently diverged genus *Salinispora* (>99% similarity in the 16S rRNA gene), we associated interspecies genetic diversity to phenotypic variation in the form of specialized metabolism. The flexible genome, which is responsible for niche and fitness differences (43), revealed species-specific signatures that were associated with BGCs and their encoded specialized metabolites (Figure 1). Species-specific genomic patterns translated to metabolite production (Figure 3A) and demonstrated that specialized metabolism can be viewed as a phylogenetically conserved trait. Broadly, our results suggest that specialized metabolites contribute to functional differences capable of promoting ecological differentiation and subsequent fine-scale diversification in microbial communities.

Previous reports in soil bacteria have shown that the production of volatile organic compounds exhibit a clear taxonomic signal (44), suggesting bacterial specialized metabolites represent conserved phylogenetic traits resembling chemotaxonomy in plants and fungi (5, 45). Similarly, we observed a distinct phylogenetic signal at both the BGC (Figure 2) and metabolite levels (Figure 3A), indicating that vertical inheritance is a major driver of BGC evolution. While horizontal gene transfer (HGT) may play a major role in expanding BGC diversity, the prevailing view that BGCs are rapidly gained and lost (46–49) remains difficult to discern given that genomic signatures (e.g., GC% and tetranucleotide bias) can be lost over time (50). As such, the time scales in which these events occur are highly relevant when considering the processes driving BGC evolution. For example, it was recently estimated that a single gene is acquired and retained through HGT every 100k years in the genus *Streptomyces* (51). By examining the distribution of BGCs among closely related *Salinispora* species, we detected a strong signal of vertical inheritance, even among BGCs that likely originated from ancient HGT events. This suggests that the collection of BGCs within *Salinispora* largely represents those that have been maintained by selection and thus produce molecules that provide a fitness advantage.

While the BGCs are largely maintained by vertical descent, the evolutionary processes driving their genetic and, ultimately, chemical diversification remain poorly understood. We observed the effects on BGC evolution at multiple levels. At the highest level, vertical descent and BGC gain/loss events largely account for the diversity and distribution of *Salinispora* BGCs. High rates of homologous recombination between closely related strains combined with barriers to interspecies transfer (due to dispersal limitation and/or genetic and ecological divergence) maintain cohesion between phylogeny and BGC distributions. At the gene cluster family (GCF) level, interspecies differences in gene composition between similar BGCs affected compound production. This was observed in both the *sta* and *sal* BGCs (Figures 4 and S10A) where different species preferentially produced different staurosporine and salinosporamide analogs. Similarly, this pattern is attributed to high rates of recombination among closely related strains, which can allow for the gain or loss of genes that encode auxiliary functions while maintaining the core biosynthetic machinery (47). Finally, at the gene level, interspecies differences in nonsynonymous SNPs within the AT_1 domain of the *salA* PKS gene were linked to the production of different analogs (Figure 4D). At this level, selection and the accumulation of genetic polymorphisms can further accelerate genetic and metabolic differentiation (52). Given that BGC evolution largely proceeds by processes of vertical descent, our results provide evidence that BGCs and the products they encode are maintained at the species level and diverge in association with speciation events. Collectively, these observations reveal that BGC evolution in *Salinispora* proceeds largely through gene gain/loss events and constrained recombination that contributes to interspecies diversity at the gene, pathway, and metabolite levels.

While genetic analyses offer insights to the evolutionary processes structuring BGC distributions, the resulting metabolite is ultimately the biological trait undergoing selection. Our observation that the collection of BGCs observed among 118 *Salinispora* genomes are largely structured by vertical inheritance suggests their products provide a selective advantage. While we did not observe strong evidence of recent selective sweeps (as indicated by reduced genetic diversity (34)), specific metabolites are fixed at the species level. This is exemplified by the production of rifamycin S by *S. arenicola* (Figure 3B). The elevated genetic diversity observed in the *rif* BGC is neutral in terms of compound production, suggesting that negative selection has removed mutations that affect the structure of the compound. In other cases, the diversity of compounds produced by a single BGC highlights the difficulty in viewing metabolic diversity as a single genotype to phenotype trait. These observations are consistent with recently proposed models of BGC evolution (53, 54) where neutral (nondirectional) processes allow for exploration of metabolic diversity while negative selection removes deleterious compounds in favor of advantageous molecules. This relaxation of purifying selection might resemble phenotypic plasticity, in the form of chemical diversity, allowing for the exploration of ecological landscapes through beneficial natural products. In this manner, BGC plasticity could facilitate the exploitation of local environmental resources through population-specific pathway evolution as an initial step in species diversification.

There is a growing appreciation that metabolite-mediated interactions can influence evolutionary fitness landscapes (53, 55). Inversely, understanding these dynamics, especially from an evolutionary perspective, can facilitate future natural product discovery efforts. Here, we show that BGC diversification had direct consequences on compound production, supporting links between specialized metabolite and species diversification. And while the rates at which BGCs are acquired via HGT remain unknown, current BGC distributions revealed species-specific signatures that are consistent with niche defining functional traits. These findings reinforce the concept that our knowledge of microbial diversity is critical for natural product discovery (56) and highlights the value of targeting rare or poorly studied taxa.

Ultimately, resolving the roles of metabolite-mediated interactions as drivers of ecological differentiation will help inform our understanding of microbial diversity and community dynamics.

MATERIALS AND METHODS

See Supplemental Information.

- Comparative genomic analyses
  - Phylogenomic and flexible genome analyses
  - BGC network and evolutionary analyses
- Metabolomics and chemical analyses
  - Strain cultivation and extraction
  - Metabolomics and mass spectometry

SUPPLEMENTAL FIGURES AND TABLES

Figure S1. Distribution of species-specific orthologous proteins.
Figure S2. Abundance of BGCs across the bacterial domain.
Figure S3. *Salinispora* BGC network and rank abundance curve
Figure S4. Pairwise average nucleotide identity (ANI) values for whole-genome comparisons and BGCs.
Figure S5. Structures of *Salinispora* specialized metabolites.
Figure S6. Phylogenies of the core genome and BGCs.
Figure S7. Recombination network based on recent gene flow in *Salinispora* genomes.
Figure S8. Selection coefficients in conserved BGC genes.
Figure S9. Representative BGCs for the *sta* and *spo* BGCs.
Figure S10. Detailed BGC architecture across all strains encoding the salinosporamide BGC.
Figure S11. Molecular network for salinosporamide production.
Figure S12. Salinosporamide AT domain phylogeny
Figure S13. Signature motifs in the active site of the AT_1 domain
Figure S14. LC/MS analysis for sporolide and salinilactam
Table S1. Characteristics of *Salinispora* strains.
Table S2. Reference information on nine BGCs.
Table S3. High-resolution MS, retention time, and predicted chemical formula for compounds associated with nine BGCs.

DATA AVAILABILITY

All genomes are publicly available (Table S1). Public datasets for all metabolomic spectra files are available at massive.ucsd.edu (MSV000085890). All other data and relevant code used can be found at https://github.com/alex-b-chase/salBGCevol.

ACKNOWLEDGEMENTS

This work was supported by the National Institute of Health (R01GM085770) to PRJ, a SIO-NIH Training Program in Marine Biotechnology fellowship to DS, and a Scripps Postdoctoral Scholar Fellowship to ABC. We thank Victoria Vasilat for assistance in culture work, Furong Sun for initial mass spectrometry quality control, Bradley S. Moore, Katherine D. Bauman, and Percival YT Chen for helpful discussions, and the Jensen Lab for thoughtful comments.

AUTHOR CONTRIBUTIONS

ABC and PRJ designed and conceptualized the research project. ABC, DS, and MNM performed culture and metabolomic experiments. DS, MNM, DGM analyzed metabolomic data. ABC analyzed genomic data and conducted statistical analyses. ABC, DS, and PRJ wrote manuscript.

REFERENCES

1. Chase AB, Gomez-Lunar Z, Lopez AE, Li J, Allison SD, Martiny AC, Martiny JBH. 2018. Emergence of soil bacterial ecotypes along a climate gradient. Environ Microbiol 20:4112–4126.
2. Johnson ZI, Zinser ER, Coe A, Mcnulty NP, Malcolm ES, Chisholm SW, Woodward EMS, Chisholm SW. 2006. Partitioning among Prochlorococcus ecotypes along environmental gradients. Science (80-) 311:1737–1740.
3. Berube PM, Rasmussen A, Braakman R, Stepanauskas R, Chisholm SW. 2019. Emergence of trait variability through the lens of nitrogen assimilation in Prochlorococcus. Elife 8:e41043.
4. Schmidt R, Ulanova D, Wick LY, Bode HB, Garbeva P. 2019. Microbe-driven chemical ecology: past, present and future. ISME J 1.
5. Pichersky E, Lewinsohn E. 2011. Convergent evolution in plant specialized metabolism. Annu Rev Plant Biol 62:549–566.
6. Thompson LR, Sanders JG, McDonald D, Amir A, Ladau J, Locey KJ, Prill RJ, Tripathi A, Gibbons SM, Ackermann G. 2017. A communal catalogue reveals Earth's multiscale microbial diversity. Nature 551:457.
7. Orsi WD, Richards TA, Francis WR. 2018. Predicted microbial secretomes and their target substrates in marine sediment. Nat Microbiol 3:32.
8. Francis CA, Tebo BM. 2002. Enzymatic manganese (II) oxidation by metabolically dormant spores of diverse Bacillus species. Appl Environ Microbiol 68:874–880.
9. Helmke E, Weyland H. 1984. Rhodococcus marinonascens sp. nov., an actinomycete from the sea. Int J Syst Evol Microbiol 34:127–138.
10. Mincer TJ, Jensen PR, Kauffman CA, Fenical W. 2002. Widespread and persistent populations of a major new marine actinomycete taxon in ocean sediments. Appl Environ Microbiol 68:5005–5011.
11. Fiedler H-P, Bruntner C, Bull AT, Ward AC, Goodfellow M, Potterat O, Puder C, Mihm G. 2005. Marine actinomycetes as a source of novel secondary metabolites. Antonie Van Leeuwenhoek 87:37–42.
12. Tuttle RN, Demko AM, Patin N, Kapono CA, Donia MS, Dorrestein P, Jensen PR. 2019. The Detection of Natural Products and Their Producers in Ocean Sediments. Appl Environ Microbiol AEM-02830.
13. Millán-Aguiñaga N, Chavarria KL, Ugalde JA, Letzel A-C, Rouse GW, Jensen PR. 2017. Phylogenomic insight into Salinispora (Bacteria, Actinobacteria) species designations. Sci Rep 7:3564.
14. Román-Ponce B, Millán-Aguiñaga N, Guillen-Matus D, Chase AB, Ginigini JGM, Soapi K, Feussner KD, Jensen PR, Trujillo ME. 2020. Six novel species of the obligate marine actinobacterium Salinispora, Salinispora cortesiana sp. nov., Salinispora fenicalii sp. nov., Salinispora goodfellowii sp. nov., Salinispora mooreana sp. nov., Salinispora oceanensis sp. nov. and Salinispora vitien. Int J Syst Evol Microbiol ijsem004330.
15. Larkin AA, Martiny AC. 2017. Microdiversity shapes the traits, niche space, and biogeography of microbial taxa. Environ Microbiol Rep 9:55–70.
16. Chase AB, Martiny JBH. 2018. The importance of resolving biogeographic patterns of microbial microdiversity. Microbiol Aust 39:5–8.
17. Patin N V, Duncan KR, Dorrestein PC, Jensen PR. 2016. Competitive strategies differentiate closely related species of marine actinobacteria. ISME J 10:478.
18. Fenical W, Jensen PR. 2006. Developing a new resource for drug discovery: marine actinomycete bacteria. Nat Chem Biol 2:666–673.
19. Ziemert N, Lechner A, Wietz M, Millán-Aguiñaga N, Chavarria KL, Jensen PR. 2014. Diversity and evolution of secondary metabolism in the marine actinomycete genus Salinispora. Proc Natl Acad Sci 201324161.
20. Letzel A, Li J, Amos GCA, Millán-Aguiñaga N, Ginigini J, Abdelmohsen UR, Gaudêncio SP, Ziemert N, Moore BS, Jensen PR. 2017. Genomic insights into specialized metabolism in the marine actinomycete Salinispora. Environ Microbiol 19:3660–3673.
21. Tidjani A-R, Lorenzi J-N, Toussaint M, van Dijk E, Naquin D, Lespinet O, Bontemps C, Leblond P. 2019. Massive gene flux drives genome diversity between sympatric Streptomyces conspecifics. MBio 10:e01533-19.
22. Freel KC, Edlund A, Jensen PR. 2012. Microdiversity and evidence for high dispersal rates in the marine actinomycete 'Salinispora pacifica.' Environ Microbiol 14:480–493.
23. Jensen PR, Williams PG, Oh D-C, Zeigler L, Fenical W. 2007. Species-specific secondary metabolite production in marine actinomycetes of the genus Salinispora. Appl Environ Microbiol 73:1146–1152.
24. Penn K, Jenkins C, Nett M, Udwary DW, Gontang EA, McGlinchey RP, Foster B, Lapidus A, Podell S, Allen EE. 2009. Genomic islands link secondary metabolism to functional adaptation in marine Actinobacteria. ISME J 3:1193.
25. Eustáquio AS, McGlinchey RP, Liu Y, Hazzard C, Beer LL, Florova G, Alhamadsheh MM, Lechner A, Kale AJ, Kobayashi Y. 2009. Biosynthesis of the salinosporamide A polyketide synthase substrate chloroethylmalonyl-coenzyme A from S-adenosyl-L-methionine. Proc Natl Acad Sci 106:12295–12300.
26. Miyanaga A, Janso JE, McDonald L, He M, Liu H, Barbieri L, Eustáquio AS, Fielding EN, Carter GT, Jensen PR. 2011. Discovery and assembly-line biosynthesis of the lymphostin pyrroloquinoline alkaloid family of mTOR inhibitors in Salinispora bacteria. J Am Chem Soc 133:13311–13313.

27. Kersten RD, Lane AL, Nett M, Richter TKS, Duggan BM, Dorrestein PC, Moore BS. 2013. Bioactivity-Guided Genome Mining Reveals the Lomaiviticin Biosynthetic Gene Cluster in Salinispora tropica. ChemBioChem 14:955–962.
28. Wilson MC, Gulder TAM, Mahmud T, Moore BS. 2010. Shared biosynthesis of the saliniketals and rifamycins in Salinispora arenicola is controlled by the sare1259-encoded cytochrome P450. J Am Chem Soc 132:12757–12765.
29. Amos GCA, Awakawa T, Tuttle RN, Letzel A-C, Kim MC, Kudo Y, Fenical W, Moore BS, Jensen PR. 2017. Comparative transcriptomics as a guide to natural product discovery and biosynthetic gene cluster functionality. Proc Natl Acad Sci 114:E11121–E11130.
30. Richter TKS, Hughes CC, Moore BS. 2015. Sioxanthin, a novel glycosylated carotenoid, reveals an unusual subclustered biosynthetic pathway. Environ Microbiol 17:2158–2171.
31. Bruns H, Crüsemann M, Letzel A-C, Alanjary M, McInerney JO, Jensen PR, Schulz S, Moore BS, Ziemert N. 2018. Function-related replacement of bacterial siderophore pathways. ISME J 12:320.
32. Udwary DW, Zeigler L, Asolkar RN, Singan V, Lapidus A, Fenical W, Jensen PR, Moore BS. 2007. Genome sequencing reveals complex secondary metabolome in the marine actinomycete Salinispora tropica. Proc Natl Acad Sci 104:10376–10381.
33. McGlinchey RP, Nett M, Moore BS. 2008. Unraveling the biosynthesis of the sporolide cyclohexenone building block. J Am Chem Soc 130:2406–2407.
34. Polz MF, Alm EJ, Hanage WP. 2013. Horizontal gene transfer and the evolution of bacterial and archaeal population structure. Trends Genet 29:170–175.
35. Eustáquio AS, Nam S, Penn K, Lechner A, Wilson MC, Fenical W, Jensen PR, Moore BS. 2011. The discovery of salinosporamide K from the marine bacterium “Salinispora pacifica” by genome mining gives insight into pathway evolution. ChemBioChem 12:61–64.
36. Feling RH, Buchanan GO, Mincer TJ, Kauffman CA, Jensen PR, Fenical W. 2003. Salinosporamide A: a highly cytotoxic proteasome inhibitor from a novel microbial source, a marine bacterium of the new genus Salinospora. Angew Chemie Int Ed 42:355–357.
37. Freel KC, Nam S-J, Fenical W, Jensen PR. 2011. Evolution of secondary metabolite genes in three closely related marine actinomycete species. Appl Environ Microbiol 77:7261–7270.
38. Goo K-S, Tsuda M, Ulanova D. 2014. Salinisporaarenicola from temperate marine sediments: new intra-species variations and atypical distribution of secondary metabolic genes. Antonie Van Leeuwenhoek 105:207–219.
39. Herbst DA, Boll B, Zocher G, Stehle T, Heide L. 2013. Structural basis of the interaction of MbtH-like proteins, putative regulators of nonribosomal peptide biosynthesis, with adenylating enzymes. J Biol Chem 288:1991–2003.
40. Polz MF, Hunt DE, Preheim SP, Weinreich DM. 2006. Patterns and mechanisms of genetic and phenotypic differentiation in marine microbes. Philos Trans R Soc B Biol Sci 361:2009 LP – 2021.
41. Thompson JR, Pacocha S, Pharino C, Klepac-Ceraj V, Hunt DE, Benoit J, Sarma-Rupavtarm R, Distel DL, Polz MF. 2005. Genotypic diversity within a natural coastal bacterioplankton population. Science (80-) 307:1311–1313.
42. Chase AB, Arevalo P, Brodie EL, Polz MF, Karaoz U, Martiny JBH. 2019. Maintenance of Sympatric and Allopatric Populations in Free-Living Terrestrial Bacteria. MBio 10:e02361-19.
43. Cordero OX, Polz MF. 2014. Explaining microbial genomic diversity in light of evolutionary ecology. Nat Rev Microbiol 12:263–273.
44. Choudoir M, Rossabi S, Gebert M, Helmig D, Fierer N. 2019. A Phylogenetic and Functional Perspective on Volatile Organic Compound Production by Actinobacteria. mSystems 4:e00295-18.
45. Lind AL, Wisecaver JH, Lameiras C, Wiemann P, Palmer JM, Keller NP, Rodrigues F, Goldman GH, Rokas A. 2017. Drivers of genetic diversity in secondary metabolic gene clusters within a fungal species. PLoS Biol 15:e2003583.
46. Fischbach MA, Walsh CT, Clardy J. 2008. The evolution of gene collectives: How natural selection drives chemical innovation. Proc Natl Acad Sci 105:4601–4608.
47. Ruzzini AC, Clardy J. 2016. Gene flow and molecular innovation in bacteria. Curr Biol 26:R859–R864.
48. Medema MH, Cimermancic P, Sali A, Takano E, Fischbach MA. 2014. A systematic computational analysis of biosynthetic gene cluster evolution: lessons for engineering biosynthesis. PLoS Comput Biol 10:e1004016.
49. Park CJ, Smith JT, Andam CP. 2019. Horizontal Gene Transfer and Genome Evolution in the Phylum Actinobacteria, p. 155–174. In Horizontal Gene Transfer. Springer.
50. Baltrus DA. 2013. Exploring the costs of horizontal gene transfer. Trends Ecol Evol 28:489–495.
51. McDonald BR, Currie CR. 2017. Lateral gene transfer dynamics in the ancient bacterial genus Streptomyces. MBio 8:e00644-17.
52. Iranzo J, Wolf YI, Koonin E V, Sela I. 2019. Gene gain and loss push prokaryotes beyond the homologous recombination barrier and accelerate genome sequence divergence. Nat Commun 10:1–10.
53. Chevrette MG, Gutiérrez-García K, Selem-Mojica N, Aguilar-Martínez C, Yañez-Olvera A, Ramos-Aboites HE, Hoskisson PA, Barona-Gómez F. 2020. Evolutionary dynamics of natural product biosynthesis in bacteria. Nat Prod Rep.
54. Fewer DP, Metsä-Ketelä M. 2020. A pharmaceutical model for the molecular evolution of microbial natural products. FEBS J 287:1429–1449.
55. Chevrette MG, Currie CR. 2019. Emerging evolutionary paradigms in antibiotic discovery. J Ind Microbiol Biotechnol 46:257–271.
56. Doroghazi JR, Albright JC, Goering AW, Ju K-S, Haines RR, Tchalukov KA, Labeda DP, Kelleher NL, Metcalf WW. 2014. A roadmap for natural product discovery based on large-scale genomics and metabolomics. Nat Chem Biol 10:963.
57. Seemann T. 2014. Prokka: rapid prokaryotic genome annotation. Bioinformatics 30:2068–2069.
58. Page AJ, Cummins CA, Hunt M, Wong VK, Reuter S, Holden MTG, Fookes M, Falush D, Keane JA, Parkhill J. 2015. Roary: rapid large-scale prokaryote pan genome analysis. Bioinformatics 31:3691–3693.
59. Sievers F, Wilm A, Dineen D, Gibson TJ, Karplus K, Li W, Lopez R, McWilliam H, Remmert M, Söding J, Thompson JD, Higgins DG. 2011. Fast, scalable generation of high-quality protein multiple sequence alignments using Clustal Omega. Mol Syst Biol 7:539.
60. Stamatakis A. 2014. RAxML version 8: A tool for phylogenetic analysis and post-analysis of large phylogenies. Bioinformatics 30:1312–1313.
61. Kanehisa M, Sato Y, Morishima K. 2016. BlastKOALA and GhostKOALA: KEGG tools for functional characterization of genome and metagenome sequences. J Mol Biol 428:726–731.
62. Blin K, Shaw S, Steinke K, Villebro R, Ziemert N, Lee SY, Medema MH, Weber T. 2019. antiSMASH 5.0: updates to the secondary metabolite genome mining pipeline. Nucleic Acids Res 47:W81–W87.
63. Navarro-Muñoz J, Selem-Mojica N, Mullowney M, Kautsar S, Tryon J, Parkinson E, De Los Santos E, Yeong M, Cruz-Morales P, Abubucker S. 2018. A computational framework for systematic exploration of biosynthetic diversity from large-scale genomic data. bioRxiv 445270.
64. Medema MH, Kottmann R, Yilmaz P, Cummings M, Biggins JB, Blin K, De Bruijn I, Chooi YH, Claesen J, Coates RC. 2015. Minimum information about a biosynthetic gene cluster. Nat Chem Biol 11:625.
65. Wattam AR, Abraham D, Dalay O, Disz TL, Driscoll T, Gabbard JL, Gillespie JJ, Gough R, Hix D, Kenyon R, MacHi D, Mao C, Nordberg EK, Olson R, Overbeek R, Pusch GD, Shukla M, Schulman J, Stevens RL, Sullivan DE, Vonstein V, Warren A, Will R, Wilson MJC, Yoo HS, Zhang C, Zhang Y, Sobral BW. 2014. PATRIC, the bacterial bioinformatics database and analysis resource. Nucleic Acids Res 42:581–591.
66. Finn RD, Clements J, Eddy SR. 2011. HMMER web server: Interactive sequence similarity searching. Nucleic Acids Res 39:29–37.
67. Angiuoli S V, Salzberg SL. 2010. Mugsy: fast multiple alignment of closely related whole genomes. Bioinformatics 27:334–342.
68. Didelot X, Wilson DJ. 2015. ClonalFrameML: efficient inference of recombination in whole bacterial genomes. PLoS Comput Biol 11:e1004041.
69. Arevalo P, VanInsberghe D, Elsherbini J, Gore J, Polz MF. 2019. A reverse ecology approach based on a biological definition of microbial populations. Cell 178:820–834.
70. Li W, Godzik A. 2006. Cd-hit: a fast program for clustering and comparing large sets of protein or nucleotide sequences. Bioinformatics 22:1658–1659.
71. Pfeifer B, Wittelsbürger U, Ramos-Onsins SE, Lercher MJ. 2014. PopGenome: an efficient Swiss army knife for population genomic analyses in R. Mol Biol Evol 31:1929–1936.
72. Kent WJ. 2002. BLAT—the BLAST-like alignment tool. Genome Res 12:656–664.
73. Schwede T, Kopp J, Guex N, Peitsch MC. 2003. SWISS-MODEL: an automated protein homology-modeling server. Nucleic Acids Res 31:3381–3385.
74. Keller A, Eng J, Zhang N, Li X, Aebersold R. 2005. A uniform proteomics MS/MS analysis platform utilizing open XML file formats. Mol Syst Biol 1.
75. Pluskal T, Castillo S, Villar-Briones A, Orešič M. 2010. MZmine 2: modular framework for processing, visualizing, and analyzing mass spectrometry-based molecular profile data. BMC Bioinformatics 11:395.
76. Clarke KR. 1993. Non-parametric multivariate analyses of changes in community structure. Austral Ecol 18:117–143.

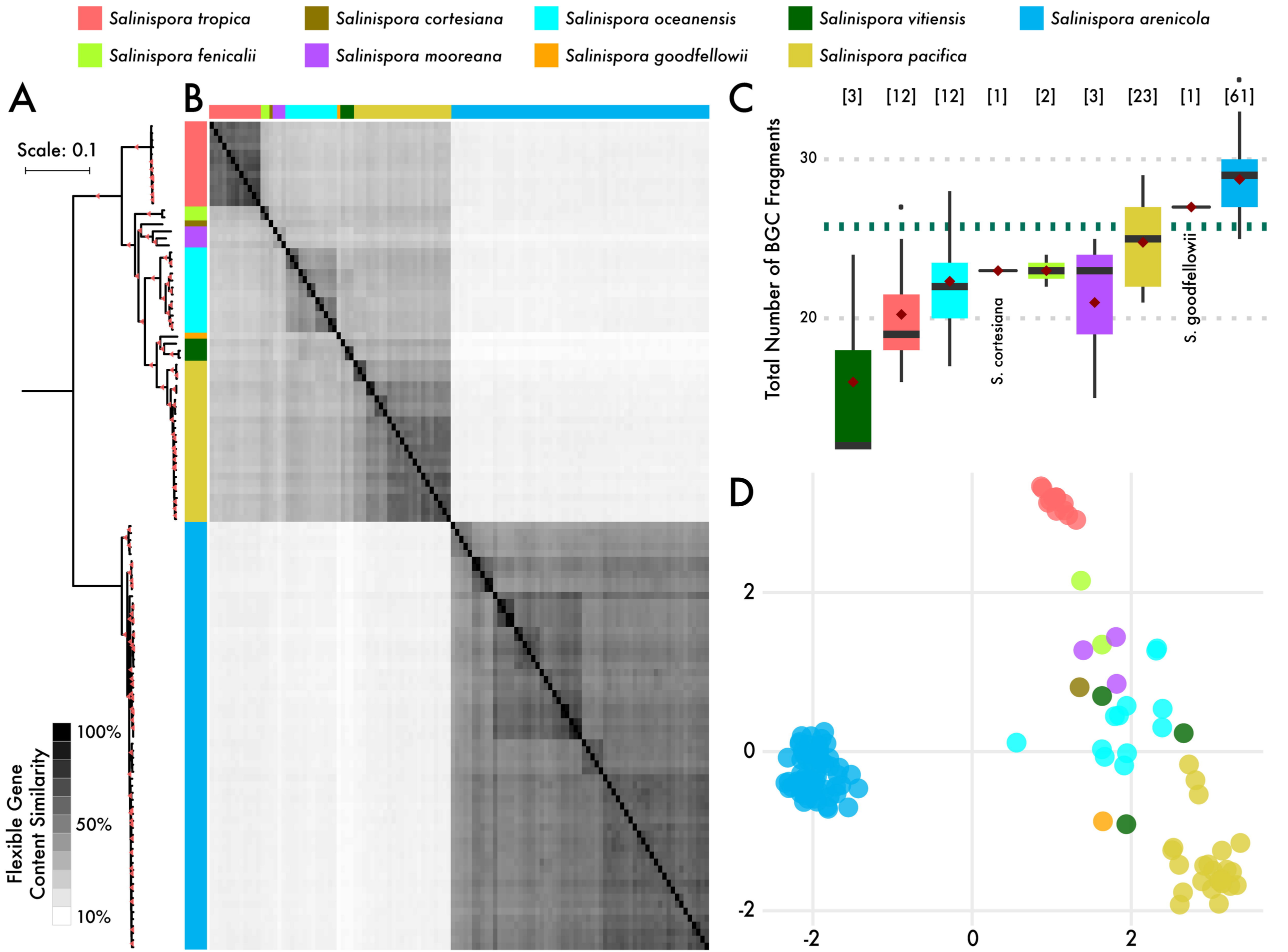
Salinispora tropica
Salinispora cortesiana
Salinispora oceanensis
Salinispora vitiensis
Salinispora arenicola
Salinispora fenicalii
Salinispora mooreana
Salinispora goodfellowii
Salinispora pacifica
A
Scale: 0.1
B
100%
50%
10%
Flexible Gene Content Similarity
C
[3]
[12]
[12]
[1]
[2]
[3]
[23]
[1]
[61]
Total Number of BGC Fragments
30
20
S. cortesiana
S. goodfellowii
D
2
0
-2
-2
0
2

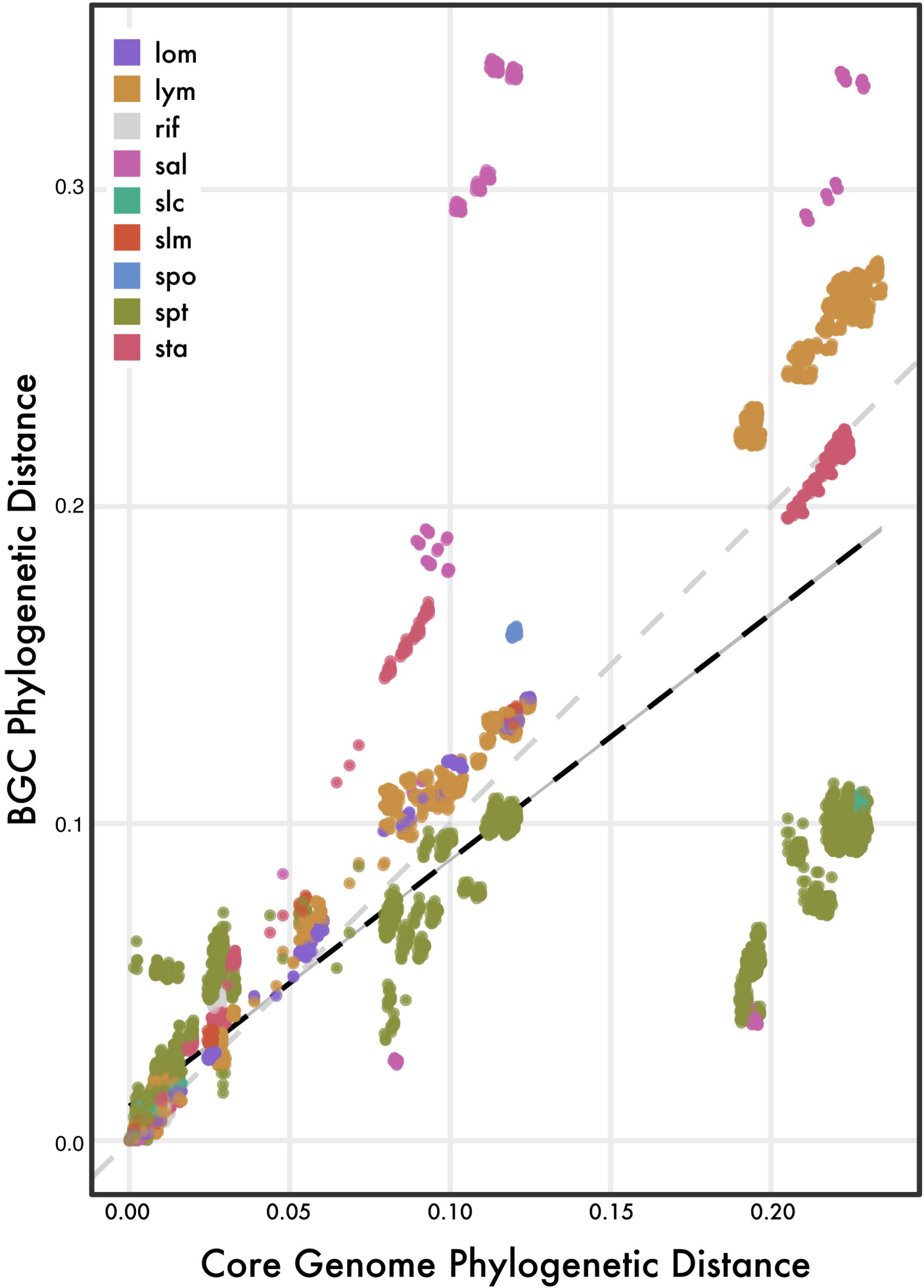
lom
lym
rif
sal
slc
slm
spo
spt
sta
0.3
0.2
0.1
0.0
BGC Phylogenetic Distance
0.00
0.05
0.10
0.15
0.20
Core Genome Phylogenetic Distance

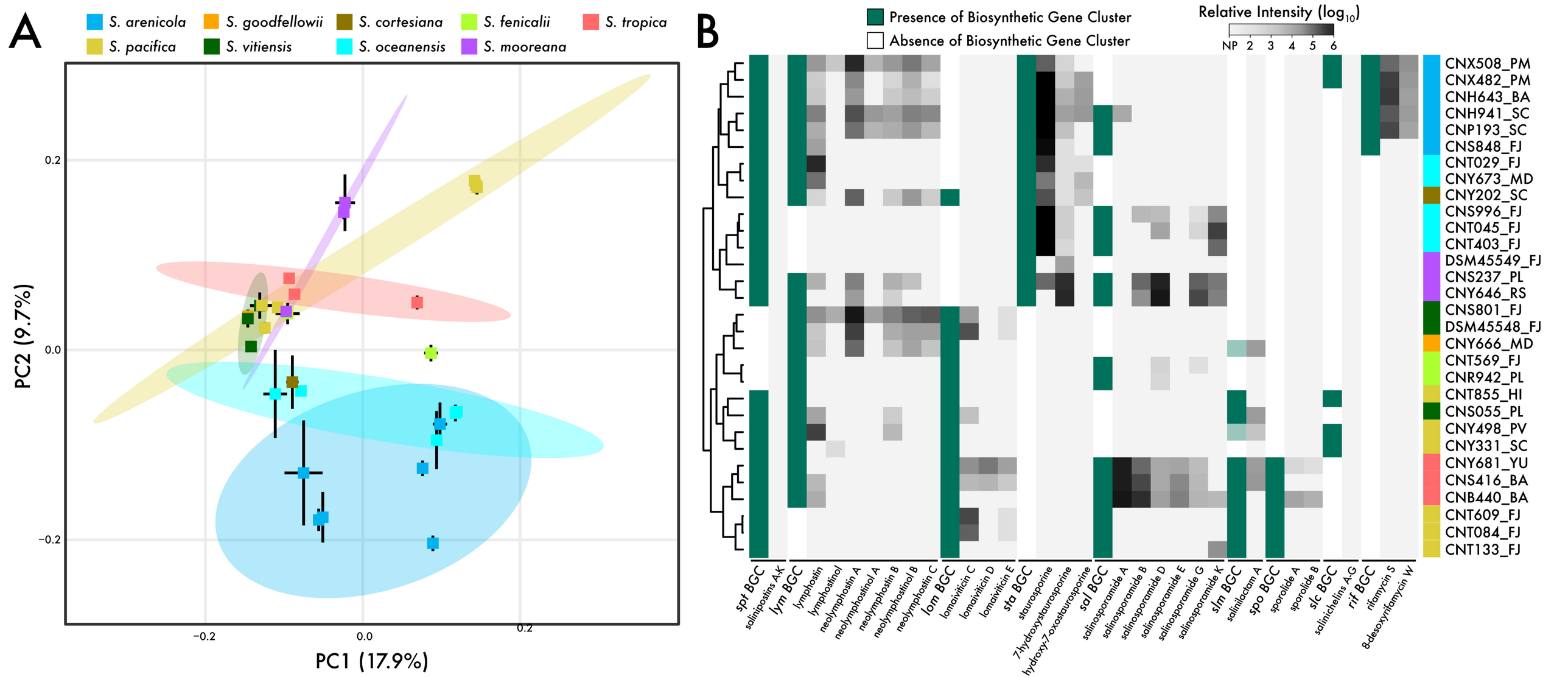
A
S. arenicola
S. goodfellowii
S. cortesiana
S. fenicalii
S. tropica
S. pacifica
S. vitiensis
S. oceanensis
S. mooreana
PC2 (9.7%)
PC1 (17.9%)
0.2
0.0
−0.2
B
Presence of Biosynthetic Gene Cluster
Absence of Biosynthetic Gene Cluster
Relative Intensity (log10)
NP 2 3 4 5 6
spt BGC
salinipostins A-K
lym BGC
lymphostin
lymphostinol
neolymphostin A
neolymphostinol A
neolymphostin B
neolymphostinol B
neolymphostin C
lom BGC
lomaiviticin C
lomaiviticin D
lomaiviticin E
sta BGC
staurosporine
7-hydroxystaurosporine
hydroxy-7-oxostaurosporine
sal BGC
salinosporamide A
salinosporamide B
salinosporamide D
salinosporamide E
salinosporamide G
salinosporamide K
slm BGC
salinilactam A
spo BGC
sporolide A
sporolide B
slc BGC
salinichelins A-G
rif BGC
rifamycin S
8-desoxyrifamycin W
CNX508_PM
CNX482_PM
CNH643_BA
CNH941_SC
CNP193_SC
CNS848_FJ
CNT029_FJ
CNY673_MD
CNY202_SC
CNS996_FJ
CNT045_FJ
CNT403_FJ
DSM45549_FJ
CNS237_PL
CNY646_RS
CNS801_FJ
DSM45548_FJ
CNY666_MD
CNT569_FJ
CNR942_PL
CNT855_HI
CNS055_PL
CNY498_PV
CNY331_SC
CNY681_YU
CNS416_BA
CNB440_BA
CNT609_FJ
CNT084_FJ
CNT133_FJ

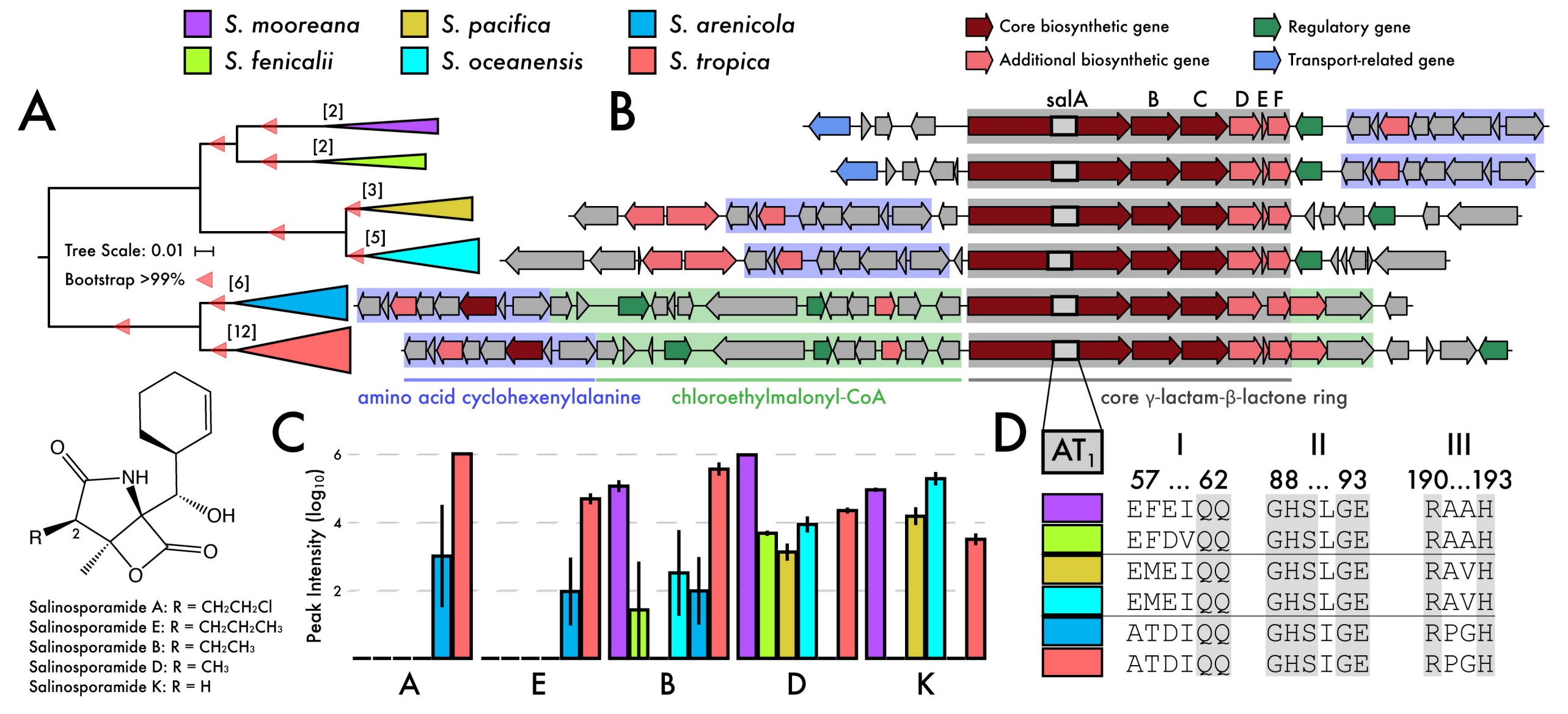
S. mooreana
S. fenicalii
S. pacifica
S. oceanensis
S. arenicola
S. tropica
Core biosynthetic gene
Additional biosynthetic gene
Regulatory gene
Transport-related gene
A
[2]
[2]
[3]
[5]
[6]
[12]
Tree Scale: 0.01
Bootstrap >99%
B
salA
B
C
D E F
amino acid cyclohexenylalanine
chloroethylmalonyl-CoA
core γ-lactam-β-lactone ring
C
Peak Intensity (log10)
6
4
2
A
E
B
D
K
D
AT1
I
II
III
57 ... 62
88 ... 93
190...193
EFEIQQ GHSLGE RAAH
EFDVQQ GHSLGE RAAH
EMEIQQ GHSLGE RAVH
EMEIQQ GHSLGE RAVH
ATDIQQ GHSIGE RPGH
ATDIQQ GHSIGE RPGH
NH
OH
O
R
2
Salinosporamide A: R = CH2CH2Cl
Salinosporamide E: R = CH2CH2CH3
Salinosporamide B: R = CH2CH3
Salinosporamide D: R = CH3
Salinosporamide K: R = H